



Detection of groundwater conditioning factors in a hilly environment

Jonmenjoy Barman¹ · F. VLH Zuali¹ · Ahmed Ali Bindajam² · Javed Mallick³ · Hazem Ghassan Abdo⁴

Received: 20 November 2023 / Accepted: 14 February 2024 / Published online: 29 March 2024
© The Author(s) 2024

Abstract

Champhai, the rice bowl of Mizoram, is known for wet rice practices. Rapid urbanization and global climate change increased the demand for groundwater. Champhai city, being a hilly township in northeast India, is very difficult to identify the potential groundwater water availability. The present study aimed at groundwater potentiality zonation in Champhai town. For these purposes ten (10) factors from topographic, climatic, hydrological and other conditions were assigned weightage based on the AHP (analytical hierarchy process) technique. The aspect was given maximum weightage as the aspect working as the controlling factors of precipitation intensity, vegetation and soil type, while LULC (land use land cover) was assigned minimum weightage that unscientific human activities reduced infiltration rate. Subsequently, an addition of ten weighted rasters was performed for groundwater potentiality zonation. As a result, it was seen that the maximum part of the study area covered low potentiality zones (31.88%), whereas high and very high potential zone covered 14.73% and 5.08, respectively. A scientific validation technique, namely AUC (area under curve) value of 0.737, denoted a good classified groundwater water potentiality zone. Further, the single-layer sensitivity analysis highlighted that elevation, slope, aspect, infiltration number, distance to streams and rainfall had the maximum effective factors based on their effective weightage. The map removal sensitivity analysis highlighted that TWI (Topographic Wetness Index) and aspect had the maximum influence on the model. However, in a hilly environment like Champhai, the output of the current study will work as a blueprint for planning and decision making.

Keywords Analytical hierarchy process · Groundwater water potentiality · Single-layer sensitivity · Map removal sensitivity

✉ Hazem Ghassan Abdo
hazemabdo@tartous-univ.edu.sy

Jonmenjoy Barman
jonmenjoybarman07@gmail.com

F. VLH Zuali
zualifanai20@gmail.com

Ahmed Ali Bindajam
abindajam@kku.edu.sa

Javed Mallick
jmallick@kku.edu.sa

¹ Department of Geography and Resource Management, Mizoram University, Aizawl 796004, India

² Department of Architecture and Planning, College of Engineering, King Khalid University, 61411 Abha, Kingdom of Saudi Arabia

³ Department of Civil Engineering, College of Engineering, King Khalid University, Abha, Kingdom of Saudi Arabia

⁴ Geography Department, Faculty of Arts and Humanities, Tartous University, P.O. Box 2147, Tartous, Syria

Introduction

Groundwater or subsurface water is very crucial for sustaining life. It is the largest freshwater reservoir in the world (Makonyo and Msabi 2021). However, it is a renewable and partially non-renewable. They are sometime confined and others unconfined, in addition to perched or artesian (Chatterjee and Purohit Ram 2009). Globally, groundwater is essential to the hydrological water cycle and to methods of water management. Nearly half of all drinking water, a third of industrial water and almost 40% of agricultural water come from underground sources (Lall et al. 2020). However, the availability or distribution of groundwater is unequally distributed over the earth due to local topography, hydrology and human activities. The disappearance of local groundwater resources can have a significant impact on the agricultural value chain, leading to large-scale migrations and economic collapse. India (251 km³/year) had the most groundwater extraction in 2010, subsequently China, the

USA, Pakistan, and Iran (63.4 km³/year), which seems to be increased in future (Abdo 2020; Rahaman et al. 2021). Rapid urbanization and global climate change make groundwater an exhausted resource. Identification of groundwater in the hilly mountains is very difficult due to its high terrain (Barman and Biswas 2022). The traditional method of groundwater exploration (drilling) is very time-consuming and manpower intensive. The development of remote sensing and GIS (geographic information system) becomes a suitable tool for groundwater availability mapping by integrating topographic, geological, hydrologic and climatic factors. Recently, statistical data-driven methods like weights of evidence (Al-abadi 2015; Boughariou et al. 2021), frequency ratio (Elmahdy and Mohamed 2014; Doke et al. 2020), evidential belief function (Mogaji and Lim 2016), logistic regression (Ozdemir 2011), artificial neural network model (Profile 2016; Lee et al. 2017), Shannon's entropy (Khoshtinat et al. 2019) are useful for groundwater availability mapping worldwide.

The identification of groundwater influencing factors in a hilly area is very crucial because of the hidden nature beneath of the ground. Several GIS intergraded models incorporating slope, elevation, aspect, distance to drainage, LULC, rainfall, distance to lineament (Pinto et al. 2017; Namous et al. 2021; Senapati and Das 2021; Rahaman et al. 2022). However, total number of thematic layers for groundwater potentiality may vary place to place based on the topographic, geological and hydrological properties (Roy et al. 2024). Previous study in the Champhai district by (Lalbiakmawia and Kumar 2017) used five thematic factors like lithology, land use land cover (LULC), slope, lineament distances and geomorphology. (Barman et al. 2023b) used a multi-criteria decision-making including slope, aspect, LULC, elevation, rainfall, river distances, precipitation concentration index (PCI), topographic wetness index (TWI), normalized difference vegetation index (NDVI), normalized difference water index (NDWI), geology and LULC. Another study by (Lalbiakmawia 2015) used GIS-based groundwater potential zonation using lithology, land use land cover (LULC), slope, lineament distances and geomorphology in Aizawl district of Mizoram. The objective of the current study is to enhance groundwater potential zonation by incorporating significant groundwater influencing factors, namely elevation, dissection index, slope, aspect, TWI, infiltration number, distance to rivers, rainfall, distance to lineaments and LULC. However, the prediction accuracy of a model may vary due to selection of appropriate conditioning factors (Sutradhar et al. 2023). Therefore, in the study, weights of the factors and domains were estimated using the analytical hierarchy process. After that judgment of the factor's weights were estimated using single-layer sensitivity analysis and map removal sensitivity analysis. Through the single-layer sensitivity analysis and map removal sensitivity

analysis the current study tried to find out most crucial factors for groundwater potentiality mapping based on their role in the study region.

The analytical hierarchy process (AHP) is a knowledge-based semi-quantitative method widely used for natural resource management (Saaty 2003). The significant advantage of the AHP method is the weightage for both factors and domains derived through a pairwise comparison matrix under a considerable consistency ratio (Abdo et al. 2023; Rahaman et al. 2022). Previously, the AHP method was used by a number of scholars (Jothibasu and Anbazhagan 2016; Arefin 2020; Shao et al. 2020; Senapati and Das 2021) for groundwater potentiality delineation, globally. Their result shows a high prediction accuracy as AHP based on the expert opinion and weight for the factors as well as the domains.

The northeastern state like Mizoram entirely covered with hilly terrain. Although rainfall is the major source of groundwater, most of the water is drained as spring water through fractures and joints (Barman and Biswas 2022; Barman et al. 2023c). It was estimated during the monsoons the rate of discharge varies from 0.002 to 0.168 m³/s, while it varies between 0.001 m³/s and 0.084 m³/s in the non-monsoon periods from the springs (Central Ground Water Board 2021). According to an abstract report of (Ground Water Resources Assessment Cell 2020) surface water in the state was found to be corresponding to depths between 8.80 and 13.25 m below ground level. The report also mentioned the groundwater level is declining at a pace of around 0.50 m per decade. The district Champhai is locally known as the 'rice bowl of Mizoram.' The district practices their own traditional jhum as well as the wet rice in the Champhai Valley facing water scarcity after the monsoon every year. According to (Central Ground Water Board 2021), the current groundwater extraction in the Champhai city area is 291,800 m³/year and the annual use of groundwater extraction for domestic use was limited to 320,600 m³/year by 2025. No such micro-level work has been published from the study area. Keeping the importance of groundwater potentiality mapping, various conditioning factors were assigned weightage by AHP methods and intergrade by weighted overlay.

Materials and methodology

About study area

Champhai city is the district headquarters of Champhai district which is located middle of the district and eastern part of Mizoram (Fig. 1). The region comes under the Indo-Burma biodiversity hotspot zone. Geographically, the township ranges between 93° 15'E and 93° 24'E longitude and 23° 32'45"N and 23° 25'15"N latitude. The real extension of

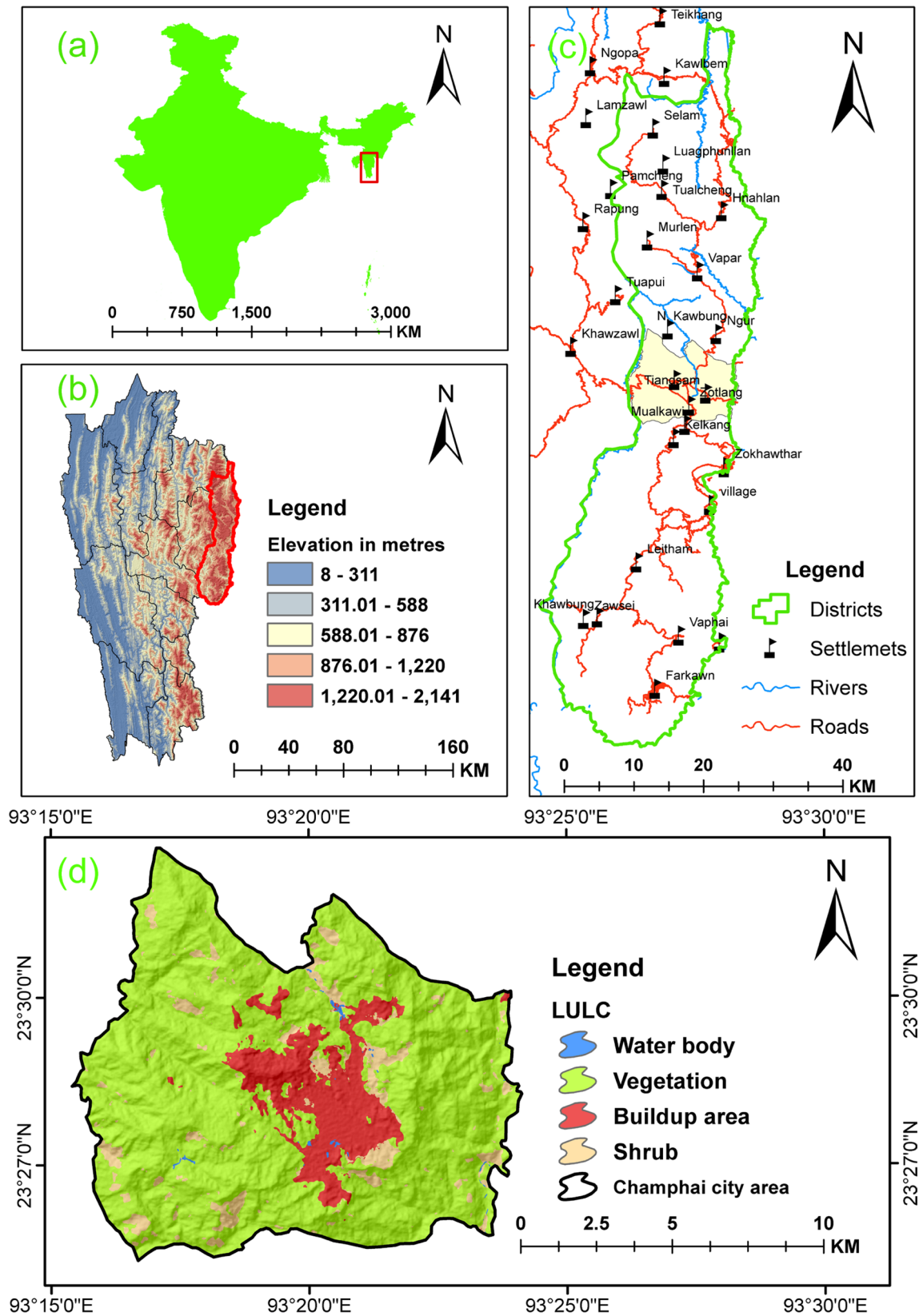


Fig. 1 Location of the study area, **a** Mizoram in India, **b** Champhai district in Mizoram, **c** Champhai city area within the district, **d** Champhai city area with spatial pattern of land use land cover

the study area is 133.15 sq. km. The township holds a total of 32,734 population with various ethnic diversity (Census of India 2011). The maximum rainfall caused by southwest monsoon ranges between 2226.84 mm/year and 2364.8 mm/year. Although the area received a good amount of precipitation, most of that washed out as surface runoff and spring water (Rao et al. 2023). The significant geomorphological feature ‘The Champhai valley’ which is known as the rice bowl of Mizoram is located in the area. Geologically the study area formed with Jenam, Laisong, and Tikak Parbat formation (Fig. 2). The Jenam formation consists of olive green, splintery shale with minor sandstone; the Laisong formation consists of sandstone, siltstone and shale, and the Laisong formation consists of sandstone, siltstone and shale with conglomerate. The tuipei, tupul and tyao are the only

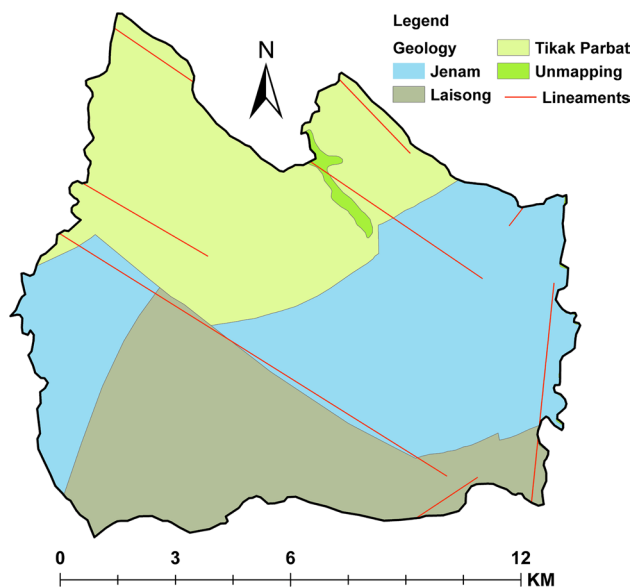


Fig. 2 Geology map of the study area (Source Geological society of India)

perennial rivers flowing through the study area. As high runoff and no rain in the winter a noticeable water scarcity is reported every year.

Database and preparation of thematic layers

The largest freshwater storage ‘groundwater’ is available in a limited environment in hilly areas (Barman et al. 2023c). The movement and storage of groundwater is depended on different topographical, hydrological, climatic and other factors. In the current study, the preparation of topographical factors was done using the ASTER digital elevation model (DEM), and hydrological factor including the drainage network was exported from ASTER DEM through threshold value ‘Flow accumulation > 300.’ In case of climatic factors average annual rainfall of 2011 to 2020 by Climate Research Unit (cru) data was used. To gather the tectonic information like ‘lineament’ by Bhukosh was used. Further, land use land cover (LULC) by ESRI 2021 was used to know the human activities over nature (Table 1). The organization of the study was generalized by methodological flow chart in Fig. 3.

The elevation is the primary groundwater potentiality controlling factor in a hilly environment (Rahaman et al. 2022). There is a revised relationship between groundwater potentiality and elevation, e.g., groundwater potentiality is maximum in the lowest elevation (Pinto et al. 2017; Namous et al. 2021; Sud et al. 2023). The elevation in the study area was classified into five classes based on the natural breaking classification system (a) 726–986 m, (b) 986.01–1171 m, (c) 1171.01–1323 m, (d) 323.01–1444 m and (e) 1444.01–1672 m. Subsequently, the dissection index (DI) is the ratio of relative relief and absolute relief. The DI ranges between 0 and 1 where 0 denoted no dissected landscape (flat topography) and 1 denoted highly dissected landscape (clip) topography (Nair et al. 2017). The lower value of DI shows minimum groundwater potentiality, while higher DI

Table 1 Description of database

Domains	Factors	Sources	Data type	Resolution
ASTER DEM	Elevation	Earthdata Search Earthdata Search (nasa.gov)	Raster	30 m
	Dissection index			
	Slope			
	Aspect			
	TWI			
	Infiltration number			
	Distance to drainage			
cru	Rainfall	High-resolution gridded datasets (uea.ac.uk)	Grided	0.5° *0.5°
Bhukosh	Distance to lineament	Bhukosh (gsi.gov.in)	Vector	NA
ESRI	LULC	Sentinel-2 10 m Land Use/Land Cover Timeseries Downloader (Mature Support)—Overview (arcgis.com)	Raster	10 m

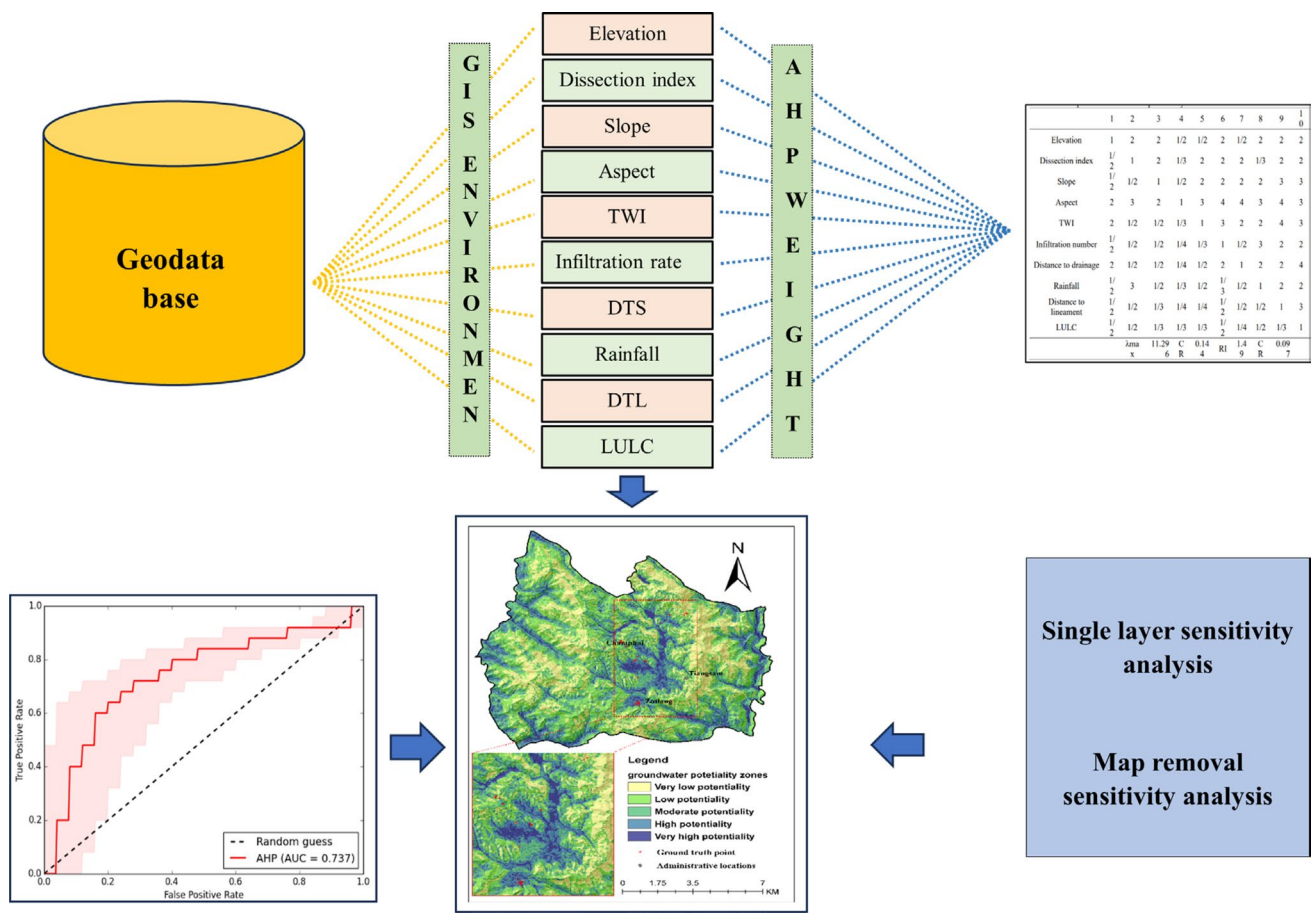


Fig. 3 Methodological flow chart

values show maximum chances of groundwater potentiality (Barman and Biswas 2022). The dissected index was classified into five classes (a) <0.05, (b) 0.06–0.1, (c) 0.11–0.15, (d) 0.16–0.2 and (e) >0.20. The slope of a region reflects the inclination or declination of the elevation of two points with respect to horizontal distance (Barman et al. 2023a). There is also a revised relationship between groundwater potentiality and slope value, i.e., chances of groundwater are decreasing with increasing the slope value (Anbarasu et al. 2020). The slope map was classified into five classes based on natural breaking classification as (a) 0–8.74°, (b) 8.75–16.8°, (c) 16.81–24.42°, (d) 24.43–32.93° and (e) 32.94–57.12°. The aspect indicated the direction of slope faces (Biswas et al. 2023). It is dominant controlling factor of vegetation types, solar radiation and precipitation (Barman and Das 2023). The aspect of the study area divided into ten classes like (a) – 1, (b) 0–22.5, (c) 22.5–67.5, (d) 67.5–112.5, (e) 112.5–157.5, (f) 157.5–202.5, (g) 202.5–247.5, (h) 247.5–292.5, (i) 292.5–337.5 and (j) 337.5–360. The TWI is the secondary morphometric index which denoted the hydrological control on topography (Razandi et al. 2015). It has been widely used for groundwater potentiality mapping

(Arulbalaji et al. 2019; Ahmad et al. 2020) and representing the spatial flow accumulation. It can be defined as Eq. (1).

$$TWI = \ln \left(\frac{A_s}{\tan \beta} \right) \tag{1}$$

where TWI is the topographic wetness index, A_s is the upslope contributing area, and β is the slope gradient. In the study, TWI was classified into five classes based on the natural breaking classification (a) 2.97–5.25, (b) 5.26–6.71, (c) 6.72–8.86, (d) 6.72–8.86 and (e) 12.04–19.12. The infiltration number is the multiply function of drainage density and stream frequency (Ghosh and Jana 2017). The infiltration number of the study area is classified into five classes (a) 0–121.63, (b) 121.64–334.47, (c) 334.48–623.33, (d) 623.34–1033.82 and (e) 1033.83–1938.42. For the distance to drainage (DTS), the potentiality of groundwater decreases with increasing distance from streams (Rahaman et al. 2022). The DTS map was produced using the Euclidean method in a GIS environment and classified into five classes (a) 0–150 m, (b) 150.01–300 m, (c) 300.01–450, (d) 450.01–600 m and (e) > 600 m. Similarly, rainfall is a significant influencing

factor for groundwater (Barman et al. 2023b). The rainfall pattern of the study area was classified into five classes (a) 2226.84–2267.96 mm, (b) 2267.97–2295.01 mm, (c) 2295.02–2320.44 mm, (d) 2320.45–2343.16 mm and (e) 2343.17–2364.8 mm. Again, the lineament distance map was produced by using the Euclidean distance method in a GIS environment and classified into five classes (a) < 300 m, (b) 300.01–600 m, (c) 600.01–900 m, (d) 900.01–1200 m and (e) > 1200 m. For groundwater potentiality land use land cover plays a significant role (Rahmati et al. 2015; Makonyo and Msabi 2021). The LULC map was classified into four major classes, namely water body, vegetation, buildup area and shrub. The thematic view of the groundwater potentiality factors is figured in Fig. 4.

Analytical hierarchy process (AHP)

The AHP is a subjective semi-quantitative approach introduced by (Saaty and Hu 1998). It is a flexible way to determine the relative weightage of a particular output (Senapati and Das 2021). The significant advantage of the approach is the power of inconsistency reduction and estimation of priority vector by pairwise comparison and decomposition (Jothibasu and Anbazhagan 2016). A pairwise comparison matrix was formed as Eq. (2) which is the primary need of the AHP method. In a town planning for groundwater potentiality zonation, ten factors (elevation, dissection index, slope, aspect, TWI, infiltration number, distance to drainage, rainfall, distance to lineament and LULC) were assigned 1 to 9 scale rating (Table 2 and 3) where 1 denotes equal importance and 9 denotes absolute significance (Table 4).

$$A = \{a_{ij}\}_{n \times n} = \begin{bmatrix} 1 & a_{12} & \dots & a_{1n} \\ a_{21} & 1 & \dots & a_{2n} \\ \vdots & \vdots & \dots & \vdots \\ a_{n1} & a_{n2} & \dots & 1 \end{bmatrix} = \begin{bmatrix} 1 & \frac{w_1}{w_2} & \dots & \frac{w_1}{w_n} \\ w_2 & 1 & \dots & \frac{w_2}{w_n} \\ \vdots & \vdots & \dots & \vdots \\ \frac{w_n}{w_1} & \frac{w_n}{w_2} & \dots & 1 \end{bmatrix} \quad (2)$$

In the second step, the matrix was converted into a normalized matrix using Eq. (3) for minimize factor dimension. It is noticeable that the matrix value of a normalized matrix ranges between 0 and 1.

$$a_{ij_{nor}} = \frac{a_{ij}}{\sum_{i=1}^n a_{ij}} \quad i, j = 1, 2, \dots, n \quad (3)$$

In the third step, the priority vector which is considered as the factor’s relative weightage was calculated as Eq. (4).

$$w_i = \left(\frac{1}{n}\right) \sum_{j=1}^n a_{ij_{nor}} \quad i = 1, 2, \dots, n \quad (4)$$

The acceptability of the comparison matrix was estimated by the consistency index (C_i) (Shao et al. 2020). However, consistency ratio (C_R) was used to calculate the consistency level. The CR is a ratio between the consistency index (C_i) and random index (R_i) (Eq. 5), where R_i was determined according to the order of the matrix (Table 5). A matrix should be accepted when the CR value is estimated below 0.1 (Biswas et al. 2023).

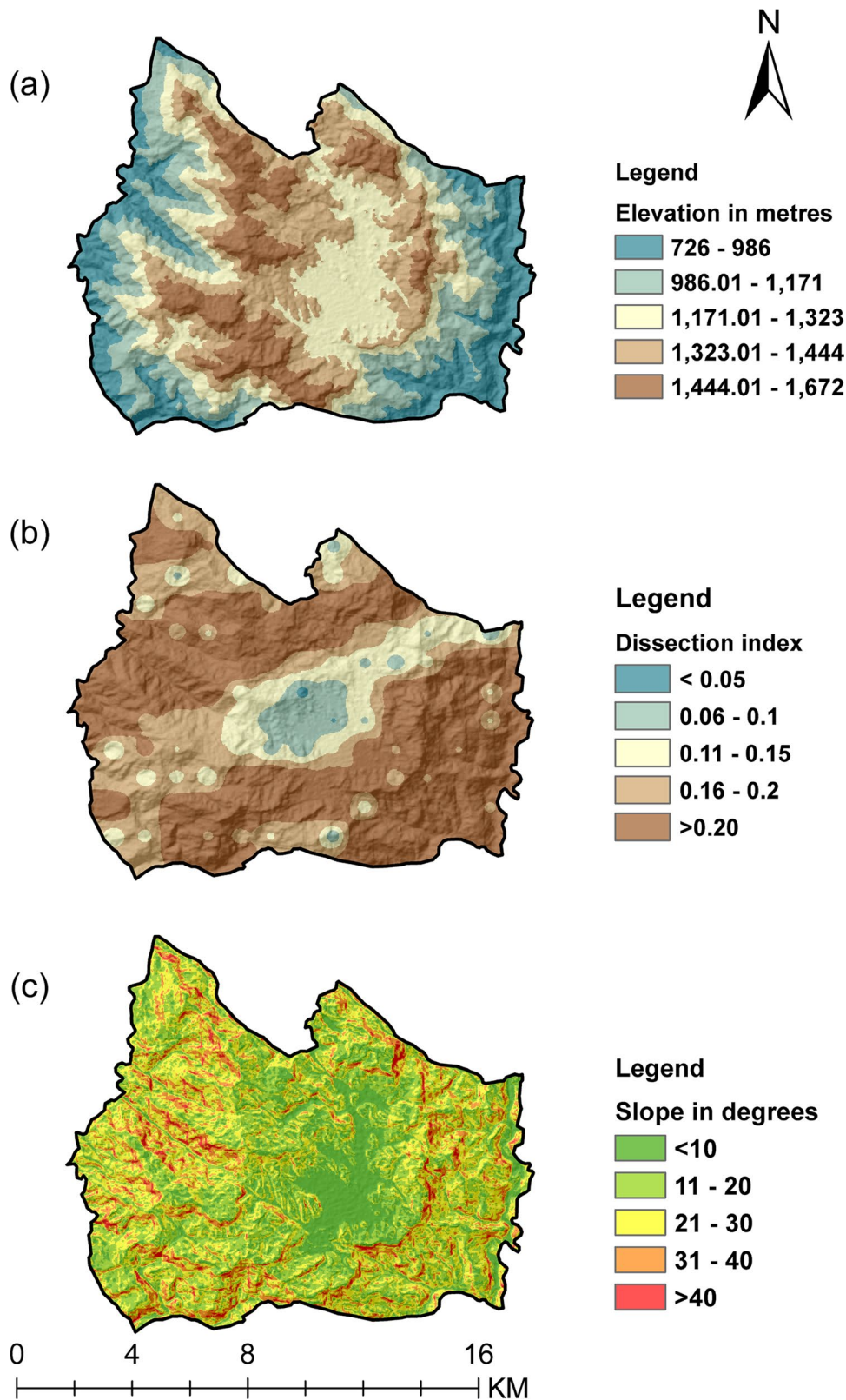
$$C_R = \frac{C_i}{R_i} \quad (5)$$

Results and discussion

Relationship between influencing factors and groundwater potentiality

The identification of groundwater potentiality zones is very difficult in hilly environments because of the high terrains (Barman et al. 2023c). In the hilly areas of Champbai town area the accessibility of groundwater is very limited due to the environmental condition (Fig. 5). The development of remote sensing and GIS opened a direction for such environmental conditions. In the present study, the relative weightage of ten (10) groundwater water-influencing conditioning factors was estimated through the AHP method. During the rating of the pairwise decision matrix, a subjective experiences and literature survey (Barman and Biswas 2022; Barman et al. 2023b) was done. The (Saaty 2005) rating was used to complete the decision matrix between the aspect and TWI; a rating of 3 was given to the aspect and 1/3 to the TWI because of aspect is more dominant than the TWI for groundwater storage. Based on the normalized weightage of the accepted decision matrix ($CR < 0.1$), the maximum and minimum weightage was given to the aspect and LULC, respectively, while others played intermediate roles. Further, for the elevation subclasses or domains, the maximum possibility of groundwater potentiality was found below 1,323. Among the five elevational subclasses, the maximum weightage was assigned to 726–986 m domains and minimum to the 1444.01–1672 m (Rahmati et al. 2015; Saranya and Saravanan 2020). For the dissection index, the maximum and minimum weights were assigned to < 0.05 and > 0.20, respectively, as the high dissection index showed a high rate of runoff (Nair et al. 2017). The flow in the gentle slope is a long duration and has larger time for infiltration, while in the steep slope, most of the rainwater flows as surface runoff; thus, the maximum and minimum weightages were given to 0–8.74 degrees and 32.94–57.12 degrees, respectively (Ahmadi et al. 2021). As the study area is

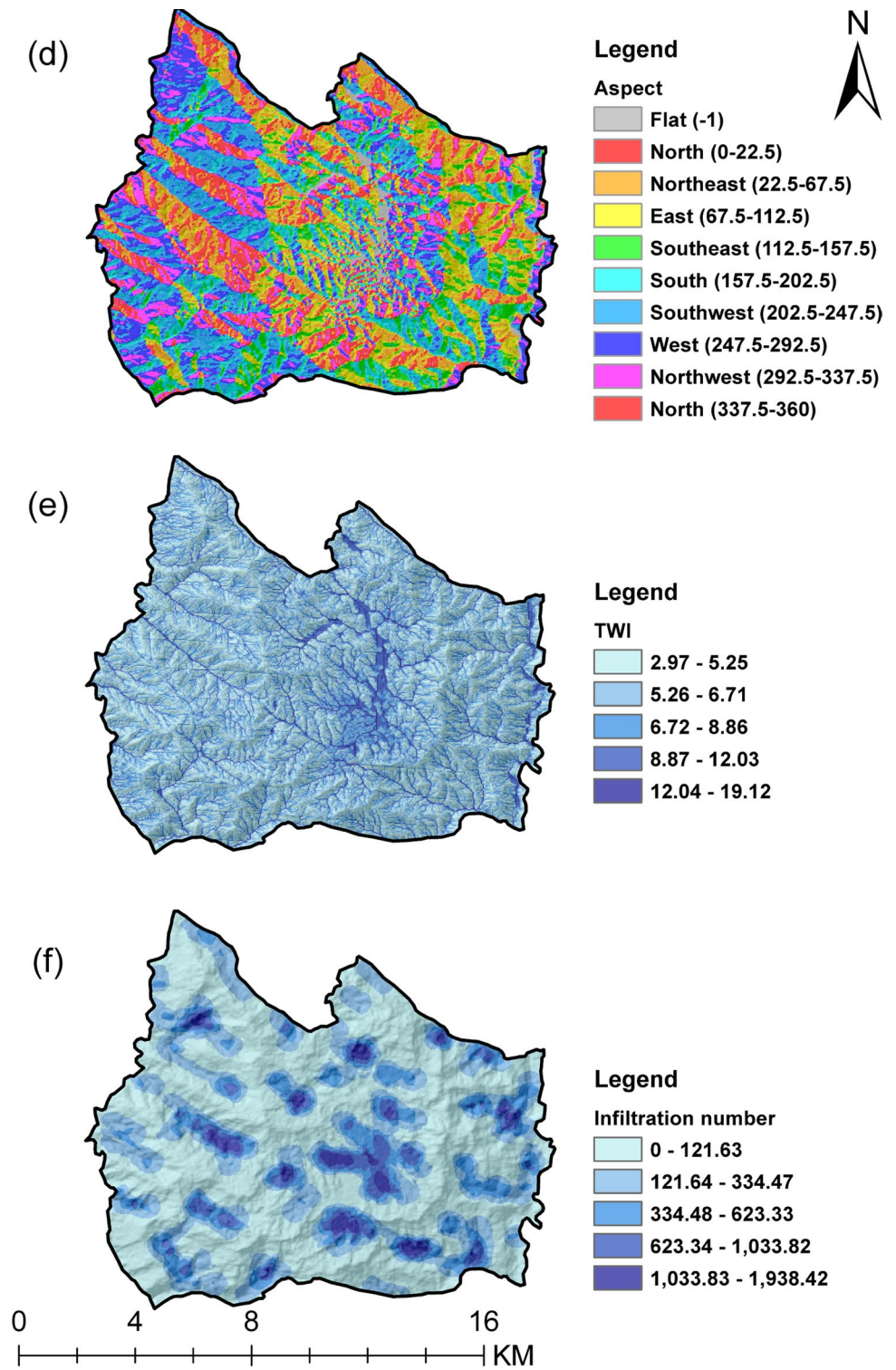
Fig. 4 Spatial distribution of subsurface water potentiality factors, **a** elevation, **b** dissection index, **c** slope, **d** aspect, **e** TWI (topographic wetness index), **f** infiltration number, **g** DTS (distance to streams), **h** rainfall, **i** DTL (distance to lineaments) and **j** LULC (land use land cover)



located in the southern part of the northern hemisphere, maximum rainfall was done by the influence of the southwest monsoon; thus, the maximum weights were given to

south, southwest and flat slope direction (Barman et al. 2023a). In the case of TWI, the maximum and minimum weights were assigned to 2.97–5.25 and 12.04–19.12,

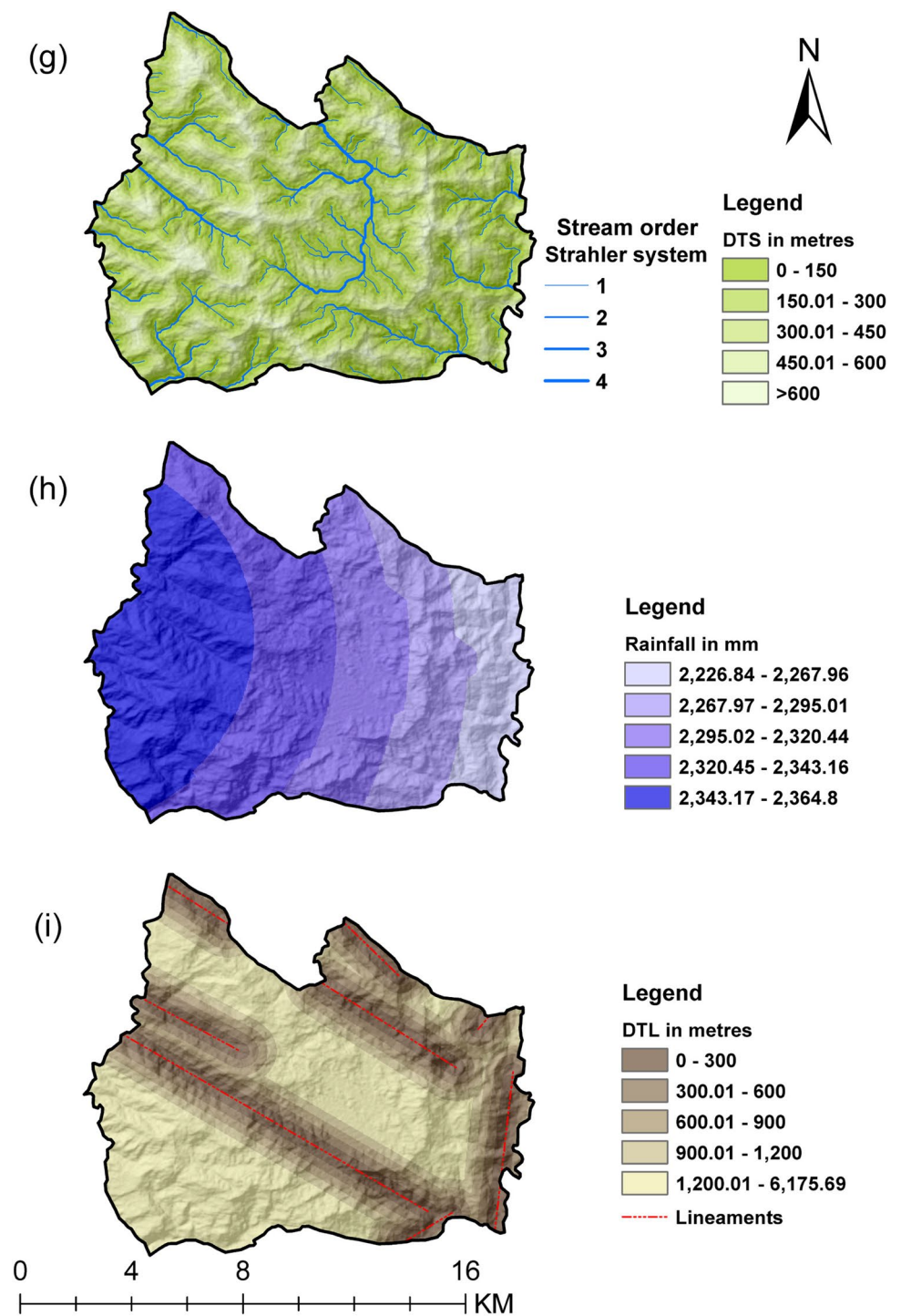
Fig. 4 (continued)



respectively, as the higher TWI value indicated more water accumulation (Razandi et al. 2015). Similarly, the maximum weightage was given to 1033.83–1938.42 and the minimum weightage to 0–121.63 for infiltration number as more infiltration denoted more groundwater storage. Regarding the DTS, a revised relationship was seen.

Near to the stream has maximum chances to maximum infiltration rate and vice versa (Saranya and Saravanan 2020). So, the maximum and minimum weightages for the DTS’s domains were assigned to 0–150 m and > 600 m, respectively. In the hilly environment rainfall is the major source for groundwater storage; thus, maximum weightage

Fig. 4 (continued)



assigned to 2343.17–2364.8 mm, and minimum weightage to 2226.84–2267.96 mm (Saranya and Saravanan 2020; Barman et al. 2023c). In case of DTL, a large quantity of groundwater wash out through lineament for the reason maximum weightage was assigned to larger distance (1200.01–6175.69 m) and minimum weightage to the shorter distance (0–300 m) (Akinwumiju et al. 2016). At least for the LULC, the maximum infiltration has had from

water body followed by vegetation cover, buildup area and shrub area; thus, the maximum weightage was given to shrub areas (Senapati and Das 2021).

Groundwater potentiality zones

An weighted sum analysis of ten (10) weighted rasters was attempted in order to produce a groundwater potentiality

Fig. 4 (continued)

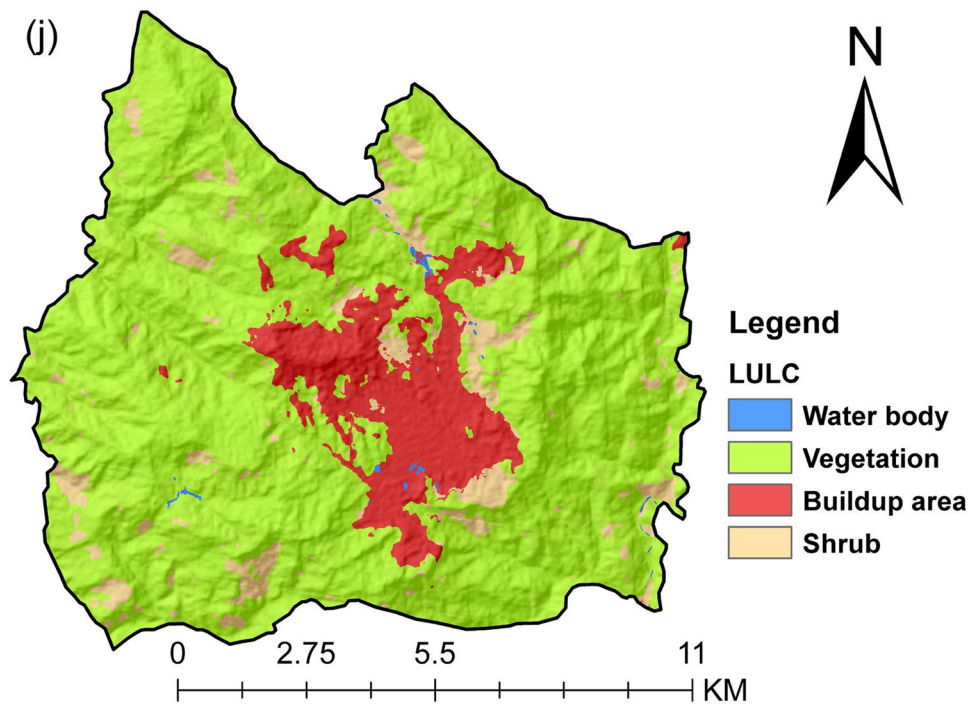


Table 2 Comparison matrix for the potentiality factors

	1	2	3	4	5	6	7	8	9	10	W_i
Elevation	1	2	2	1/2	1/2	2	1/2	2	2	2	0.11
Dissection index	1/2	1	2	1/3	2	2	2	1/3	2	2	0.11
Slope	1/2	1/2	1	1/2	2	2	2	2	3	3	0.12
Aspect	2	3	2	1	3	4	4	3	4	3	0.22
TWI	2	1/2	1/2	1/3	1	3	2	2	4	3	0.12
Infiltration number	1/2	1/2	1/2	1/4	1/3	1	1/2	3	2	2	0.07
Distance to drainage	2	1/2	1/2	1/4	1/2	2	1	2	2	4	0.10
Rainfall	1/2	3	1/2	1/3	1/2	1/3	1/2	1	2	2	0.08
Distance to lineament	1/2	1/2	1/3	1/4	1/4	1/2	1/2	1/2	1	3	0.05
LULC	1/2	1/2	1/3	1/3	1/3	1/2	1/4	1/2	1/3	1	0.04
		λ_{max}	11.296	CR	0.144	RI	1.49	CR	0.097		

map as Eq. (6). The raster value range between 0.11 and 0.29 denoted the upper limit and lower limit of groundwater potentiality.

$$W_{\text{subsurface}} = \text{Elevation}_{\text{AHP}} + \text{DI}_{\text{AHP}} + \dots + \text{LULC}_{\text{AHP}} \quad (6)$$

To better understand the groundwater potentiality, the study area was zoned into five hierarchical zones based on the natural breaking classification system. The hierarchical zones are, namely very high potential, high potential, moderate potential, low potential and very low potential zones (Fig. 6). As per the model, only 5.08% of the study area had a very high potential for groundwater, whereas the maximum part of the study area came under low potential for groundwater (31.88%). The other zones, namely

high potential, moderate potential and very low potential zones, covered 14.73%, 25.34% and 22.98% of the total area, respectively (Fig. 7). The geographical distribution of very high potential zones concentrated mainly along the rivers due to high infiltration, low elevation, high TWI value, low dissection and low slope (Roy et al. 2024). On the contradictory, very low potential zones were found mainly along the ridge due to high elevation and low infiltration (Arulbalaji et al. 2019; Rajesh and Jobin 2019). The low potential area was located mainly on a steep slope due to high runoff (Mukherjee et al. 2012). In the case of moderate and high potential zones, those were concentrated 150–450 m from the rivers and between 1000- and 1500-m elevation.

Table 3 Comparison matrix and weightage for the domains

Elevation	1	2	3	4	5	6	7	8	9	10	W_i
726–986	1	4	4	3	2						0.420
986.01–1171	1/4	1	2	3	3						0.231
1171.01–1323	1/4	1/2	1	2	2						0.147
1323.01–1444	1/3	1/3	1/2	1	1						0.094
1444.01–1672	1/4	1/3	1/2	1	1						0.108
			CI	0.092	RI	1.12	CR	0.082			
<i>Dissection index</i>											
<0.05	1	3	3	3	2						0.393
0.06–0.1	1/3	1	2	2	1						0.191
0.11–0.15	1/3	1/2	1	2	1						0.148
0.16–0.2	1/3	1/2	1/2	1	1						0.112
>0.20	1/2	1	1	1	1						0.156
			CI	0.039	RI	1.12	CR	0.035			
<i>Slope</i>											
0–8.74	1	4	4	3	2						0.420
8.75–16.8	1/4	1	2	3	3						0.231
16.81–24.42	1/4	1/2	1	2	2						0.147
24.43–32.93	1/3	1/3	1/2	1	1						0.094
32.94–57.12	1/2	1/3	1/2	1	1						0.108
			CI	0.092	RI	1.12	CR	0.082			
<i>Aspect</i>											
–1	1	2	2	2	2	3	3	2	3	3	0.193
0–22.5	1/2	1	1	2	3	1/2	1/2	3	1/2	1/2	0.094
22.5–67.5	1/2	1	1	1/2	1/2	1/2	1/2	1	1	2	0.067
67.5–112.5	1/2	1/2	2	1	1	1	1	1	1	2	0.089
112.5–157.5	1/2	1/3	2	1	1	1/2	1/2	1/2	1/2	1/2	0.061
157.5–202.5	1/3	2	2	1	2	1	4	3	3	3	0.158
202.5–247.5	1/3	2	2	1	2	1/4	1	3	3	3	0.123
247.5–292.5	1/2	1/3	1	1	2	1/3	1/3	1	1/2	1/2	0.059
292.5–337.5	1/3	2	1	1	2	1/3	1/3	2	1	1/2	0.077
337.5–360	1/3	2	1/2	1/2	2	1/3	1/3	2	2	1	0.079
			CI	0.140	RI	1.49	CR	0.094			
<i>TWI</i>											
2.97–5.25	1	1/2	1/2	1/2	1/2						0.108
5.26–6.71	2	1	1/2	1/2	1/3						0.129
6.72–8.86	2	2	1	1/2	1/3						0.167
6.72–8.86	2	2	2	1	1/2						0.231
12.04–19.12	2	3	3	2	1						0.365
			CI	0.056	RI	1.12	CR	0.050			
<i>Infiltration number</i>											
0–121.63	1	1/2	1/2	1/2	1/2						0.108
121.64–334.47	2	1	1/2	1/2	1/3						0.129
334.48–623.33	2	2	1	1/2	1/3						0.167
623.34–1033.82	2	2	2	1	1/2						0.231
1033.83–1938.42	2	3	3	2	1						0.365
			CI	0.056	RI	1.12	CR	0.050			
<i>DTS</i>											
0–150	1	2	2	3	3						0.369
150.01–300	1/2	1	1	2	2						0.208
300.01–450	1/2	1	1	1	2						0.183
450.01–600	1/3	1/2	1	1	1						0.129

Table 3 (continued)

Elevation	1	2	3	4	5	6	7	8	9	10	W_i
> 600	1/3	1/2	1/2	1	1						0.110
			CI	0.014	RI	1.12	CR	0.012			
<i>Rainfall</i>											
2226.84–2267.96	1	1/2	1/3	1/3	1/2						0.086
2267.97–2295.01	2	1	1/3	1/3	1						0.138
2295.02–2320.44	3	3	1	1/3	1						0.227
2320.45–2343.16	3	3	3	1	1						0.342
2343.17–2364.8	2	1	1	1	1						0.206
			CI	0.076	RI	1.12	CR	0.068			
<i>DTL</i>											
0–300	1	1/2	1/2	1/2	1/2						0.108
300.01–600	2	1	1/2	1/2	1/3						0.129
600.01–900	2	2	1	1/2	1/3						0.167
900.01–1200	2	2	2	1	1/2						0.231
1200.01–6175.69	2	3	3	2	1						0.365
			CI	0.056	RI	1.12	CR	0.050			
<i>LULC</i>											
Water body	1	1	2	3							0.356
Vegetation	1	1	2	2							0.325
Buildup area	1/2	1/2	1	2							0.194
Shrub	1/3	1/2	1/2	1							0.125
			CI	0.015	RI	0.9	CR	0.017			

Table 4 Comparison scale after Saaty (1970)

No	Scale	Description
1	1	Equally preferred
2	3	Moderately preferred
3	5	Strongly preferred
4	7	Very strongly preferred
5	9	Extremely important
6	Intermediate (2, 4, 6, 8)	Preferences made halfway between the main integers

Validation

A map is not useful without proper validation (Barman et al. 2023a; Biswas et al. 2023). The receiver operating characteristic curve (ROC) and area under curve (AUC) are the scientific validation techniques for groundwater potentiality mapping. The graphical plot of ROC consists of a ‘True Positive Rate’ in the ‘Y-axis’ and a ‘False Positive Rate’ in the ‘X-axis.’ The ‘True Positive Rate’ denoted the proportion of borehole points

correctly classified as very and highly potential zones in the prediction map. The ‘False Positive Rate’ rate described the proportion of non-bore hole points correctly classified as low and very low potential zones in the prediction map (Barman et al. 2023a). In the current study, 25 borehole points by Gramin GPS were marked for validation purposes. An ArcGIS extension ‘ArcSDM’ was used for the preparation of the ROC curve (Fig. 8a). The AUC value of 0.737 indicated a good classified groundwater potentiality zone (Al-abadi 2015). As a spatial distribution, 48% (12 points) of the bore hole points fall into the high potentiality zone, 16% (4 points) fall in both very potentiality and moderate potentiality zones, 12% (3 points) fall in low potentiality zones, and only 8% (2 points) fall in very low potentiality zone. Figure 8b shows a scatter plot of groundwater potentiality, water extraction and well depth. In the “Z”-axis the groundwater potentiality was plotted ranging from 1 to 5, in which 1 denoted very low potentiality and 5 denoted very high potentiality. It also indicated that most of the boreholes are located in high and very high potentiality zones. Similarly, the “X” and “Y”-axis indicated maximum boreholes had a depth of less than 210 ft and weekly groundwater extraction was more than 3500 Liters/week, respectively.

Table 5 Random index value

n	1	2	3	4	5	6	7	8	9	10
RI	0	0	0.58	0.9	1.12	1.24	1.32	1.41	1.45	1.51

Fig. 5 Field photographs



It is highlighted that local residences benefit from groundwater in both the winter and summer seasons (Table 6).

Sensitivity analysis

The subjective way of weightage selection of the parametric test is an undesirable part (Dadgar et al. 2017). That significantly impacts the model outcome. The sensitivity analysis is a scientific technique to estimate the importance of each influencing factor to groundwater potentiality (Awawdeh et al. 2013). Two well-known tests, namely single-layer sensitivity analysis and map removal sensitivity analysis, were performed for the current study. The single-layer sensitivity shows the effective weight of each influencing factor for the

groundwater potentiality. Mathematically, the single-layer sensitivity can be calculated as Eq. (7).

$$SL_{\text{sensi}} = \frac{M_{wi}R_{cl}}{W_{\text{subsurface}}} * 100 \quad (7)$$

where SL_{sensi} is the single-layer sensitivity index, M_{wi} is the empirical weight of factor (s), R_{cl} is the rating of the factors, and $W_{\text{subsurface}}$ is the groundwater potentiality. Based on the sensitivity index, the maximum effective weightage was seen for the slope (mean variation 14.24%) followed by DTS, elevation, aspect and rainfall in the study area (Table 7). It was followed by TWI, dissection index, LULC, infiltration number and DTL (Fig. 9). The empirical weightage for DTS was estimated at 11%, whereas the estimated effective weight was seen at 13.62%. For the aspect, the empirical and effective weightage was calculated at 22% and 11.94%;

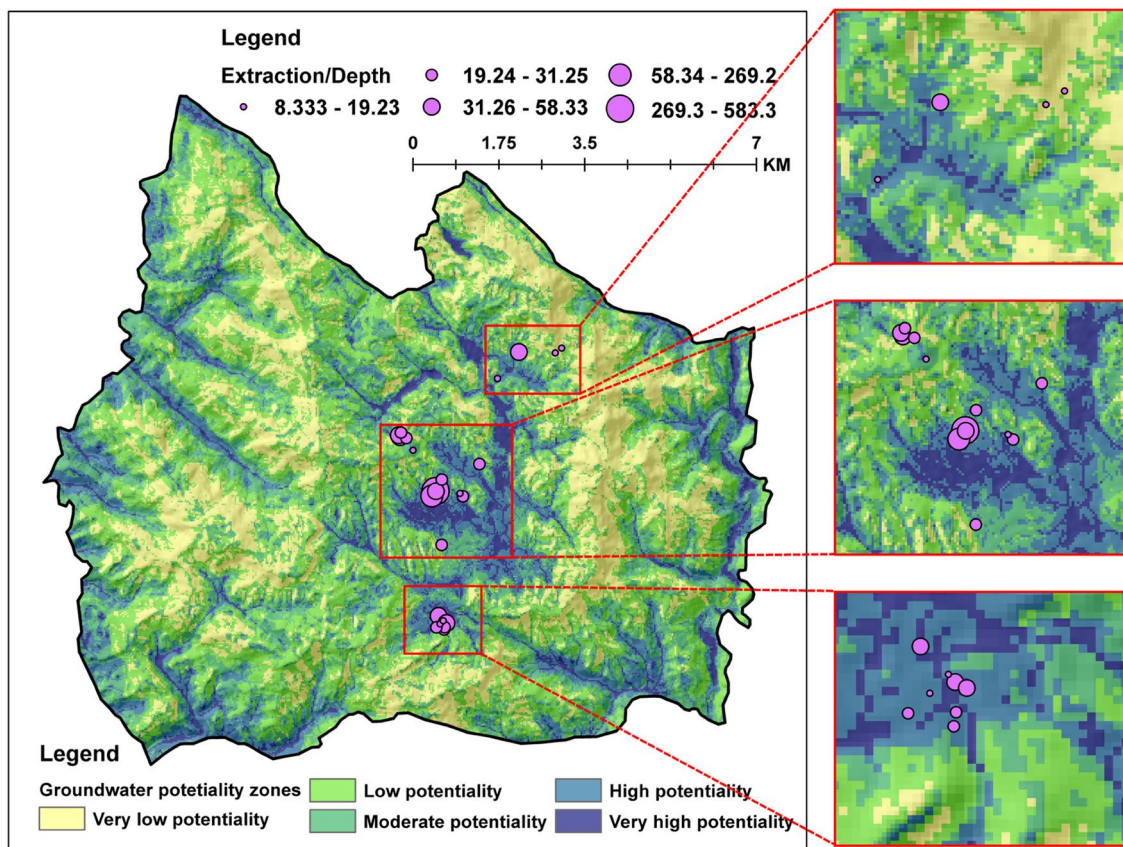


Fig. 6 Groundwater potentiality zones of the study area with distribution of wells where larger proportional circle indicated more potential

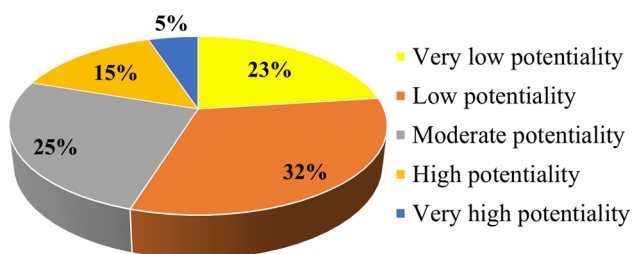


Fig. 7 Areal extension of groundwater potentiality zones

hence, a big deviation was observed. The difference between empirical and effective weightage was less or more similar for the elevation, dissection index, slope, IN, TWI, DTS, rainfall, DTL and LULC (Table 7).

The map removal sensitivity examines the importance of a factor for groundwater potentiality. It can be estimated as Eq. (8).

$$MR_{sensi} = \frac{\left| \left(\frac{W_{subsurface}}{N} \right) - \left(\frac{W_{subsurface'}}{n} \right) \right|}{W_{subsurface}} * 100 \tag{8}$$

where MR_{sensi} denotes map removal sensitivity index, $W_{subsurface}$ is the groundwater potentiality map including all factors, and $W_{subsurface}'$ is the groundwater potentiality map excluding factor. Further, N and n denote the number of factors for $W_{subsurface}$ and $W_{subsurface}'$ modeling, respectively. In the current study, no significant changes were seen after removing a single factor. The TWI and aspect were found sensitive factors with the mean sensitivity index (SI) variation of 10.009% and 2.256, respectively. On the contradictory, LULC, rainfall, DTS and slope had less influence in the model (Table 8).

The groundwater potentiality zone after map removed is figured in Fig. 10. The high potentiality area was increased by map removal after elevation, DI, slope, aspect, TWI, rainfall and LULC. The maximum change was observed after the removal of TWI followed by LULC, rainfall and DTS (Table 9). The area of high potentiality was decreased by the removal of IN and DTL. Similarly, the modeled estimated area of high potentiality was 19.48 Sq. Km, while the maximum area was increased after the removal of TWI followed by LULC, DI, DTS and aspect and the area was decreased by the removal of IN followed by slope, elevation, DTL and rainfall. The moderate potential area was increased by the removal of rainfall, slope and DI and decreased after

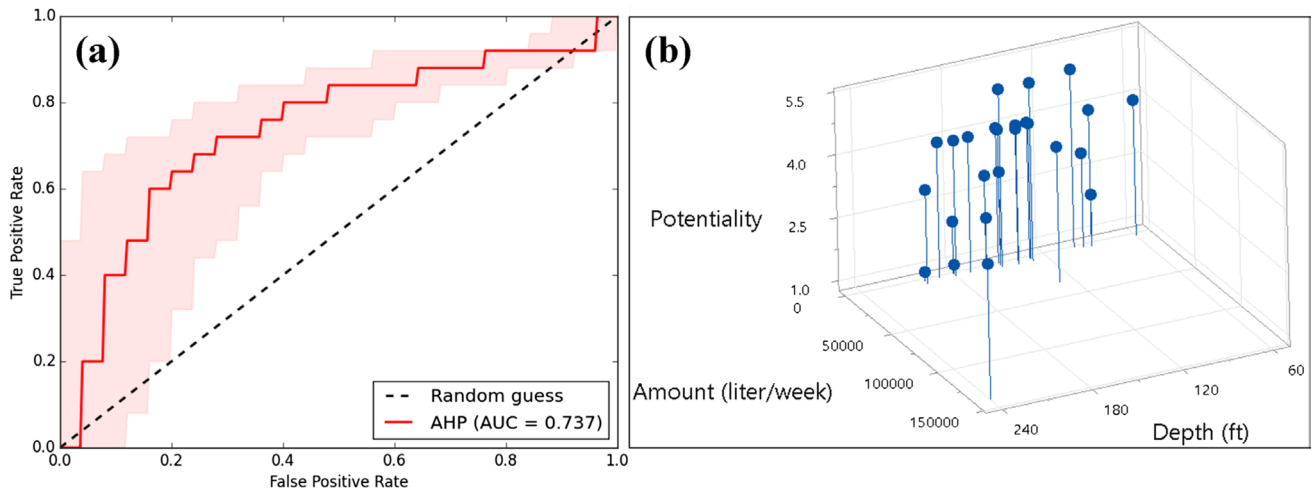


Fig. 8 Model’s prediction accuracy; **a** receiver operating characteristic curve and **b** 3D scatter plot of groundwater potentiality vs amount of groundwater extraction and well depth

Table 6 Depth and water extraction from boreholes

Latitude	Longitude	Depth (ft)	Extraction (Liter/week)
23.4821	93.327633	95	3500
23.4818	93.32785	90	4100
23.4826	93.328083	160	4500
23.4816	93.32915	160	5000
23.4709	93.334233	130	35,000
23.4739	93.3362	200	6000
23.4714	93.33985	130	2500
23.4708	93.340433	130	4000
23.4768	93.343717	150	3800
23.4974	93.351667	90	4700
23.4981	93.3602	200	3500
23.4972	93.358917	180	2500
23.4925	93.347367	100	1500
23.4794	93.3305	180	1500
23.4463	93.336617	180	4500
23.4467	93.33505	138	3000
23.4488	93.335483	130	6000
23.4467	93.3367	170	4000
23.4479	93.336433	150	1400
23.4477	93.336667	60	3500
23.4475	93.337067	150	5500
23.4473	93.3358	190	3000
23.4718	93.335017	140	7000
23.4718	93.334967	240	140,000
23.4619	93.33615	150	3600

Source Authors primary survey

Table 7 Descriptive statistics of single-layer sensitivity analysis

Thematic layers	Empirical weightage (%)	SI variation (%)			
		Min	Max	Mean	SD
Elevation	11	3.71	32.07	12.21	6.42
Dissection index (DI)	11	4.31	25.33	9.26	1.79
Slope	12	4.78	31.76	14.24	5.76
Aspect	22	4.93	26.91	11.94	3.95
TWI	12	5.32	24.57	9.81	2.42
Infiltration number (IN)	7	2.65	16.47	5.32	1.53
Distance to streams (DTS)	10	4.78	26.58	13.62	4.38
Rainfall	8	2.37	20.90	10.08	3.86
Distance to lineament (DTL)	5	1.75	13.77	4.38	2.01
LULC	4	1.75	10.41	6.59	1.75

removal of elevation, aspect, TWI, IN, DTL and LULC. Further, the low potential area was increased than the model estimated area after removal of slope, aspect, IN, DTL and elevation, DI, TWI, DTS, rainfall and LULC. The low potential area was decreased after the removal of DI, slope, TWI, DTS, rainfall and LULC, and the area was increased after the removal of elevation, aspect, In and DTL.

Conclusion

The present study aimed to zonation of groundwater potential zonation of the district headquarters of Champhai district. In this regard, eight factors were assigned weighted using the subjective AHP method under a certain consistency ratio (less than 0.1). The maximum and minimum weightage were assigned to aspect and LULC,

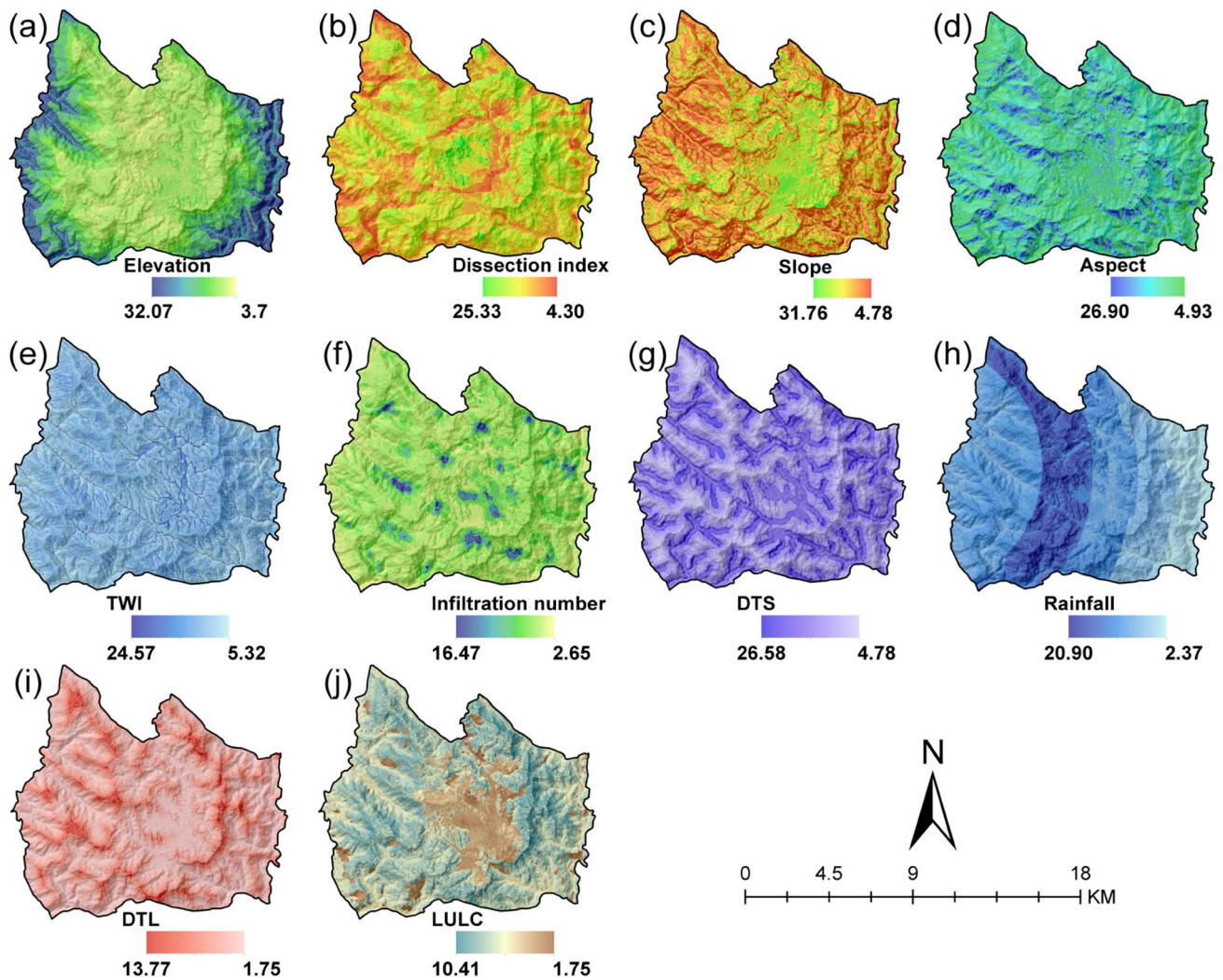


Fig. 9 Effective weight of groundwater potentiality factors, **a** elevation, **b** dissection index, **c** slope, **d** aspect, **e** TWI (topographic wetness index), **f** infiltration number, **g** DTS (distance to streams), **h** rainfall, **i** DTL (distance to lineaments) and **j** LULC (land use land cover)

Table 8 Descriptive statistics of map removal sensitivity analysis

Thematic layers	SI variation (%)			
	Min	Max	Mean	SD
Elevation	0.000	1.885	0.986	0.454
Dissection index	0.000	2.676	0.864	0.364
Slope	0.000	1.826	0.695	0.416
Aspect	0.219	3.402	2.256	0.565
TWI	6.463	21.868	10.009	1.896
Infiltration number	1.896	1.351	0.928	0.189
Distance to drainage	0.000	1.444	0.472	0.266
Rainfall	0.000	1.506	0.560	0.347
Distance to lineament	0.000	1.239	0.845	0.246
LULC	0.000	1.261	0.401	0.236

respectively. After all, ten weighted rasters were integrated with the ArcGIS environment to produce a groundwater potential map. To better understand, the generated raster groundwater map was classified into five categories very low potentiality, low potentiality, moderate potentiality, high potentiality and very high potentiality using a natural breaking classification system. As a spatial distribution, only 5.08% of the area had a very high potential for groundwater. The result showed that the river valley in the eastern part of the state was excellent for groundwater potentiality. The same was seen for the western part of the study area. The central part of the study area is known heart of the district; the main residential area was good for groundwater potentiality. The other parts of the study area characteristics were low and very low for groundwater potentiality mainly due to the presence of ridge. The AUC value of 0.737 indicated a good classified groundwater

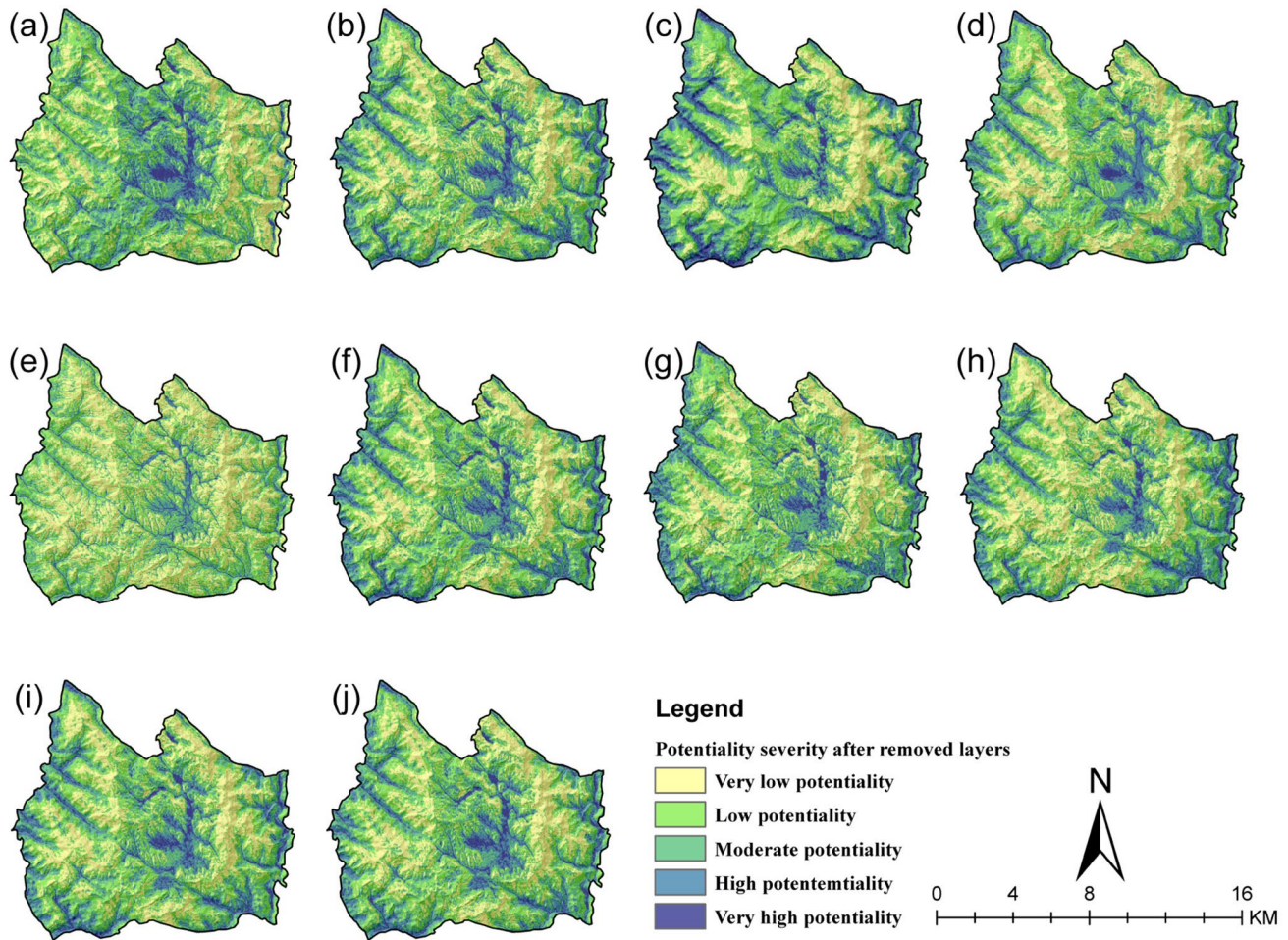


Fig. 10 Groundwater potentiality zone after removed single factors, **a** removed elevation, **b** removed dissection index, **c** removed slope, **d** removed aspect, **e** removed TWI (topographic wetness index), **f**

removed infiltration number, **g** removed DTS (distance to streams), **h** removed rainfall, **i** DTL (distance to lineaments) and **j** removed LULC (land use land cover)

Table 9 Areal changes of potentiality zones after removed single layers

Subsurface water potentiality	Elevation	DI	Slope	Aspect	TWI	IN	DTS	Rainfall	DTL	LULC	Model area
Very low potential	58.39	8.63	24.79	31.59	4.09	44.83	28.91	18.24	31.79	10.96	30.40
Low potential	25.67	32.57	43.12	43.36	12.46	55.08	37.47	33.48	48.63	22.55	42.17
Moderate potential	25.29	47.24	41.53	28.03	26.76	22.33	25.58	40.80	32.21	30.62	33.52
High potential	11.64	35.87	10.21	19.57	47.92	7.47	22.34	18.47	15.09	40.62	19.48
Very high potential	11.29	7.87	12.65	9.74	41.07	2.57	17.99	21.30	4.57	27.53	6.71

NB: All the areas are in Km²

DI dissection index, TWI topographic wetness index, IN infiltration number, DTS distance to streams, DTL distance to lineaments, LULC land use land cover

potentiality zonation. The sensitivity analysis of single-layer sensitivity highlighted effective weight of slope, elevation, aspect, DTS and rainfall was higher than 10%. Subsequently, the map removal sensitivity analysis showed that TWI and aspect have their maximum influence of 10.009% and 2.256%, respectively.

Acknowledgements Authors thankfully acknowledge the Deanship of Scientific Research for proving administrative and financial supports. Funding for this research was given under award numbers RGP2/411/44 by the Deanship of Scientific Research; King Khalid University, Ministry of Education, Kingdom of Saudi Arabia

Author contributions JB, FVZ and AAB helped in conceptualization and supervision; JB, FVZ, AAB, JM and HGA contributed to writing—review and editing; JB, FVZ, AAB and HGA were involved in data curation and formal analysis; JB, FVZ, JM and HGA helped in evidence collection, review and editing. All authors read and approved the final manuscript.

Funding Authors thankfully acknowledge the Deanship of Scientific Research for proving administrative and financial supports. Funding for this research was given under award numbers RGP2/411/44 by the Deanship of Scientific Research; King Khalid University, Ministry of Education, Kingdom of Saudi Arabia.

Data availability Data used in the manuscript will be available from various open sources. The DEM data were downloaded from Earthdata Search | Earthdata Search (nasa.gov); Rainfall from High-resolution gridded datasets (uea.ac.uk); Lineament information from Bhukosh (gsi.gov.in); and LULC from Sentinel-2 10 m Land Use/Land Cover Timeseries Downloader (Mature Support)—Overview (arcgis.com).

Declarations

Conflict of interest The authors have no conflicts of interest to declare.

Open Access This article is licensed under a Creative Commons Attribution 4.0 International License, which permits use, sharing, adaptation, distribution and reproduction in any medium or format, as long as you give appropriate credit to the original author(s) and the source, provide a link to the Creative Commons licence, and indicate if changes were made. The images or other third party material in this article are included in the article's Creative Commons licence, unless indicated otherwise in a credit line to the material. If material is not included in the article's Creative Commons licence and your intended use is not permitted by statutory regulation or exceeds the permitted use, you will need to obtain permission directly from the copyright holder. To view a copy of this licence, visit <http://creativecommons.org/licenses/by/4.0/>.

References

- Abdo HG (2020) Evolving a total-evaluation map of flash flood hazard for hydro-prioritization based on geohydromorphometric parameters and GIS–RS manner in Al-Hussain river basin Tartous Syria. *Nat Hazards* 104(1):681–703. <https://doi.org/10.1007/s11069-020-04186-3>
- Abdo HG, Aljohani THD, Almohamad H, Al-Dughairi AA, Al-Mutiry M (2023) Sanitary municipal landfill site selection by integration of GIS and multi-criteria techniques for environmental sustainability in Safita area Tartous governorate Syria. *Environ Sci Pollut Res* 30(11):30834–30854. <https://doi.org/10.1007/s11356-022-24287-9>
- Ahmad I, Dar MA, Teka AH, Teshome M (2020) GIS and fuzzy logic techniques-based demarcation of groundwater potential zones: a case study from Jemma River basin, Ethiopia. *J Afr Earth Sci* 169:103860. <https://doi.org/10.1016/j.jafrearsci.2020.103860>
- Ahmadi H, Kaya OA, Babadagi E et al (2021) GIS-based groundwater potentiality mapping using AHP and. *Environ Sci Proc* 5:1–15
- Akinwumiju AS, Olorunfemi MO, Afolabi O (2016) GIS-based integrated groundwater potential assessment of Osun drainage Basin, Southwestern Nigeria. *Ife J Sci* 18:147–168
- Al-Abadi AM (2015) Groundwater potential mapping at northeastern Wasit and Missan governorates, Iraq using a data-driven weights of evidence technique in framework of GIS. *Environ Earth Sci.* <https://doi.org/10.1007/s12665-015-4097-0>
- Anbarasu S, Brindha K, Elango L (2020) Multi-influencing factor method for delineation of groundwater potential zones using remote sensing and GIS techniques in the western part of Perambalur district, southern India. *Earth Sci Inf* 13:317–332. <https://doi.org/10.1007/s12145-019-00426-8>
- Arefin R (2020) Groundwater potential zone identification using an analytic hierarchy process in Dhaka City, Bangladesh. *Environ Earth Sci* 79:1–16. <https://doi.org/10.1007/s12665-020-09024-0>
- Arulbalaji P, Padmalal D, Sreelash K (2019) GIS and AHP techniques based delineation of groundwater potential zones: a case study from Southern Western Ghats, India. *Sci Rep* 9:1–17. <https://doi.org/10.1038/s41598-019-38567-x>
- Awawdeh M, Obeidat M, Al-mohammad M (2013) Integrated GIS and remote sensing for mapping groundwater potentiality in the Tulul al Ashaqif. Northeast Jordan. <https://doi.org/10.1007/s12517-013-0964-8>
- Barman J, Biswas B (2022) Application of e-TOPSIS for groundwater potentiality zonation using morphometric parameters and geospatial technology of Vanvate Lui Basin, Mizoram, NE India. *J Geol Soc India* 98:1385–1394. <https://doi.org/10.1007/s12594-022-2186-8>
- Barman J, Ali SS, Biswas B, Das J (2023a) Application of index of entropy and Geospatial techniques for landslide prediction in Lunglei district, Mizoram, India. *Nat Hazards Res.* <https://doi.org/10.1016/j.nhres.2023.06.006>
- Barman J, Durjoy D, Soren L et al (2023b) Preference selection index and geospatial technique for groundwater potentiality zonation in Aizawl district, Mizoram. *Transactions* 45:67–82
- Barman J, Das P (2023) A multi-criteria decision-making approach for land suitability assessment for tea cultivation in Hilly Aizawl district in Mizoram, India. In: Das J, Halder S (eds) *Advancement of GI-science and sustainable agriculture*. (1st edn). Springer Nature, Switzerland, p 135
- Barman J, Soren DDL, Roy S, et al (2023c) Preference selection index and geospatial technique for groundwater potentiality zonation in Aizawl district, Mizoram, India. *Transactions* 45
- Biswas B, Rahaman A, Barman J (2023) Comparative assessment of FR and AHP models for landslide susceptibility mapping for Sikkim, India and preparation of suitable mitigation techniques. *J Geol Soc India* 99:791–801. <https://doi.org/10.1007/s12594-023-2386-x>
- Boughariou E, Allouche N, Ben BF et al (2021) Delineation of groundwater potentials of Sfax region, Tunisia, using fuzzy analytical hierarchy process, frequency ratio, and weights of evidence models. *Environ Dev Sustain.* <https://doi.org/10.1007/s10668-021-01270-x>
- Census of India (2011) Office of the registrar general & census commissioner, India. Ministry Of Home Affairs, Government of India, New Delhi
- Central Ground Water Board (2021) Dynamic ground water resources Chatterjee R, Purohit Ram R (2009) Estimation of replenishable groundwater resources of India and their status of utilization. *Curr Sci Assoc* 96:1581–1591
- Dadgar MA, Zeaieanfrouzabadi P, Dashti M (2017) Extracting of prospective groundwater potential zones using remote sensing data, GIS, and a probabilistic approach in Bojnourd basin, NE of Iran. *Arab J Geosci.* <https://doi.org/10.1007/s12517-017-2910-7>
- Doke A, Pardeshi SD, Das S (2020) Drainage morphometry and groundwater potential mapping : application of geoinformatics with frequency ratio and influencing factor approaches. *Environ Earth Sci.* <https://doi.org/10.1007/s12665-020-09137-6>
- Elmahdy SI, Mohamed MM (2014) Probabilistic frequency ratio model for groundwater potential mapping in Al Jaww plain. UAE. <https://doi.org/10.1007/s12517-014-1327-9>
- Ghosh PK, Jana NC (2017) Groundwater potentiality of the Kumari River Basin in drought-prone Purulia upland, Eastern India: a

- combined approach using quantitative geomorphology and GIS. *Sustain Water Resour Manag* 4:583–599. <https://doi.org/10.1007/s40899-017-0142-3>
- Ground Water Resources Assessment Cell (2020) Ground water depletion survey report
- Jothibasu A, Anbazhagan A (2016) Modeling groundwater probability index in Ponnaiyar River basin of South India using analytic hierarchy process. *Model Earth Syst Environ* 2:1–14. <https://doi.org/10.1007/s40808-016-0174-y>
- Khoshtinat S, Aminnejad B, Hassanzadeh Y, Ahmadi H (2019) Groundwater potential assessment of the Sero plain using bivariate models of the frequency ratio, Shannon entropy and evidential belief function. *J Earth Syst Sci*. <https://doi.org/10.1007/s12040-019-1155-0>
- Lalbiakmawia F (2015) Application of remote sensing and GIS techniques for ground water potential zones Mapping in Aizawl district, Mizoram, India. *Int J Eng Sci Res Technol* 4:292–299
- Lalbiakmawia F, Kumar S (2017) Ground water prospecting using remote sensing and GIS in Champhai district, Mizoram, India. In: Sati VP, Lalmalsawmzauva KC (eds) *Natural resources management for sustainable development and rural livelihoods*, 1st edn. Today & Tomorrow's Printers and Publishers, New Delhi, pp 151–165
- Lall U, Josset L, Russo T (2020) A snapshot of the world's groundwater challenges. *Ann Rev Environ Resour* 45:171–196
- Lee S, Hong S, Jung H (2017) GIS-based groundwater potential mapping using artificial neural network and support vector machine models: the case of Boryeong city in Korea. *Geocarto Int* 6049:0–1. <https://doi.org/10.1080/10106049.2017.1303091>
- Makonyo M, Msabi MM (2021) Remote sensing applications: society and environment identification of groundwater potential recharge zones using GIS-based multi-criteria decision analysis: a case study of semi-arid midlands Manyara fractured aquifer, North-Eastern Tanzania. *Remote Sens Appl Soc Environ* 23:100544. <https://doi.org/10.1016/j.rsase.2021.100544>
- Mogaji KA, Lim HS (2016) Development of groundwater favorability map using GIS-based driven data mining models: an approach for effective groundwater resource management. Taylor & Francis, Routledge
- Mukherjee P, Singh CK, Mukherjee S (2012) Delineation of groundwater potential zones in arid region of India—a remote sensing and GIS approach. *Water Resour Manag* 26:2643–2672. <https://doi.org/10.1007/s11269-012-0038-9>
- Nair HC, Padmalal D, Joseph A, Vinod PG (2017) Delineation of groundwater potential zones in river basins using geospatial tools—an example from Southern Western Ghats, Kerala, India. *J Geovis Spat Anal* 1:1–16. <https://doi.org/10.1007/s41651-017-0003-5>
- Namous M, Hssaisoune M, Pradhan B et al (2021) Spatial prediction of groundwater potentiality in large semi-arid and karstic mountainous region using machine learning models. *Water* 13:2273. <https://doi.org/10.3390/w13162273>
- Ozdemir A (2011) Using a binary logistic regression method and GIS for evaluating and mapping the groundwater spring potential in the Sultan Mountains (Aksehir, Turkey). *J Hydrol* 405:123–136. <https://doi.org/10.1016/j.jhydrol.2011.05.015>
- Pinto D, Shrestha S, Babel MS, Ninsawat S (2017) Delineation of groundwater potential zones in the Comoro watershed, Timor Leste using GIS, remote sensing and analytic hierarchy process (AHP) technique. *Appl Water Sci* 7:503–519. <https://doi.org/10.1007/s13201-015-0270-6>
- Profile SEE (2016) Delineating groundwater potential zones in Western Cameroon Highlands using GIS based artificial neural networks model and remote sensing data. *Int J Innov Appl Stud* 15(4):747
- Rahaman H, Reman S, Ahmed R, Sajjad H (2021) Exploring carrying capacity of water and its potential sources in Imphal city, Manipur. In: Singh AL, Jamal S (eds) *Water supply for the urban poor in Indian cities*. B.R. Publishing Corporation, Delhi
- Rahaman A, Biswas B, Barman J et al (2022) Delineation of groundwater potential zones through AHP: a case study from Tamil Nadu, India. In: Das J, Kumar BS (eds) *Monitoring and managing multi-hazards*, 1st edn. Springer Nature, Switzerland, pp 317–325
- Rahmati O, Samani AN, Mahdavi M et al (2015) Groundwater potential mapping at Kurdistan region of Iran using analytic hierarchy process and GIS. *Arab J Geosci* 8:7059–7071. <https://doi.org/10.1007/s12517-014-1668-4>
- Rajesh ALA, Jobin R (2019) Mapping of groundwater recharge potential zones and identification of suitable site-specific recharge mechanisms in a tropical river Basin. *Earth Syst Environ*. <https://doi.org/10.1007/s41748-019-00138-5>
- Rao KS, Barman BK, Sandipan N et al (2023) Morphometry-based prioritization of watersheds for soil and water conservation measures: a case study on Vanvate Lui basin, Mizoram, North-East India Koduri. *Arab J Geosci* 16:279. <https://doi.org/10.1007/s12517-023-11353-w>
- Razandi Y, Pourghasemi HR, Neisani NS (2015) Application of analytical hierarchy process, frequency ratio, and certainty factor models for groundwater potential mapping using GIS. *Earth Sci Inf* 8:867–883. <https://doi.org/10.1007/s12145-015-0220-8>
- Roy KC, Barman J, Biswas B (2024) Groundwater for Sustainable Development Multi-criteria decision-making for groundwater potentiality zonation in a groundwater scarce region in central India using methods of compensatory aggregating functions. *Groundw Sustain Dev* 25:101101. <https://doi.org/10.1016/j.gsd.2024.101101>
- Saaty TL (2003) Decision-making with the AHP: why is the principal eigenvector necessary. *Eur J Oper Res* 145:85–91
- Saaty TL (2005) Making and validating complex decisions with the AHP/ANP. *J Syst Sci Syst Eng* 14:1–36
- Saaty TL, Hu G (1998) Ranking by eigenvector versus other methods in the analytic hierarchy process. *Appl Math Lett* 11:121–125. [https://doi.org/10.1016/S0893-9659\(98\)00068-8](https://doi.org/10.1016/S0893-9659(98)00068-8)
- Saranya T, Saravanan S (2020) Groundwater potential zone mapping using analytical hierarchy process (AHP) and GIS for Kancheepuram District , Tamilnadu , India. *Model Earth Syst Environ*. <https://doi.org/10.1007/s40808-020-00744-7>
- Senapati U, Das TK (2021) Assessment of basin-scale groundwater potentiality mapping in drought-prone upper Dwarakeshwar River basin, West Bengal, India, using GIS-based AHP techniques. *Arab J Geosci* 14(11):960
- Shao Z, Huq E, Cai B et al (2020) Integrated remote sensing and GIS approach using Fuzzy-AHP to delineate and identify groundwater potential zones in semi-arid Shanxi. *Environ Model Softw* 134:104868. <https://doi.org/10.1016/j.envsoft.2020.104868>
- Sud A, Kanga R, Singh SK et al (2023) Simulating groundwater potential zones in mountainous Indian Himalayas—a case study of Himachal Pradesh Anshul. *Hydrology*. <https://doi.org/10.3390/hydrology10030065>
- Sutradhar C, Poddar D, Das J (2023) Optimization of conditioning factors for groundwater potential zonation using GIS-based single parameter and map removal sensitivity analysis in Alipurduar district of West Bengal, India. *Model Earth Syst Environ*. <https://doi.org/10.1007/s40808-023-01859-3>

Publisher's Note Springer Nature remains neutral with regard to jurisdictional claims in published maps and institutional affiliations.